Sensors and Materials, Vol. 14, No. 1 (2002) 047–056
MYU Tokyo

S & M 0469

Pt Electrode-Based Sensor Prepared by Metal Organic Chemical Vapor Deposition for Oxygen Activity Measurements in Glass Melts

Roberto Vargas-García, Antonio Romero-Serrano, Miguel Angeles-Hernandez, Federico Chavez-Alcala and Carlos Gomez-Yañez

Metallurgy and Materials Department, IPN-ESIQIE, A. Postal 75-874, Mexico D.F. 07300

(Received May 11, 2001; accepted September 17, 2001)

Key words: metal organic chemical vapor deposition, oxygen sensor, Pt film, glass melts

A sensor employing yttria-stabilized zirconia (YSZ) was used to determine the oxygen activity of amber glass at laboratory scale at temperatures from 1473 K to 1673 K. The YSZ sensors were coated with Pt electrode films deposited by the metal organic chemical vapor deposition (MOCVD) method to increase the conductivity of the measuring devices and to diminish their response time. The oxygen potential of glass was related to the oxidation state of iron through the Nernst equation and the free energy of the equilibrium reaction between FeO and Fe_2O_3. The oxidation reduction in the FeO-Fe_2O_3 equilibrium moved towards the reduced side when the temperature of molten glass was increased. A strong correlation of the activity ratio (aFeO$_{1.5}$/aFeO) to the R_2O/C parameter (where R = Na and K) was found at all of the test temperatures.

1. Introduction

Many properties of glass products such as colour, visco-elastic behavior and surface tension depend strongly on their oxidation state. Therefore, over the last few years, in situ oxidation state control systems have been installed in working chambers and feeder channels for the continuous measurement of the oxidation state in the glass industry in order to control the properties of the final glass product. Most of these in situ techniques are based on the electrochemical determination of the oxygen activity in the glass melt by

using yttria-stabilized zirconia (YSZ) as an oxygen ion conductor.[1–3]

The YSZ sensors have also been successfully used to measure gases in air such as CO, SO_2 and NO_x at relatively low temperatures (600–650°C).[4,5] Platinum is widely used as the electrode material in these sensors because of its electro-catalytic nature which promotes the charge transfer reactions at the electrolyte/electrode interface. Usually, porous Pt electrodes are prepared by firing Pt paste at around 900–1200°C; however, highly catalytic Pt electrodes can also be prepared by an appropriate deposition technique (sputtering or CVD) on the surface of the solid electrolyte.[6] It has been shown that the highly catalytic Pt electrodes improve the response time of the sensor.[7]

Several empirical parameters such as redox numbers have also been reported for the measurement of the oxidation state of the glass in industrial furnaces.[8,9] However, these numbers do not give sufficient information to control the oxidation state of the glass since they cannot take into account the nonequilibrium state of melts in industrial plants.

In this work we have prepared YSZ sensors to estimate the oxygen activity in glass melts. In order to improve the efficiency and the response time of these oxygen sensors, Pt electrode films were prepared by the MOCVD technique. We also introduce the (R_2O/C) parameter ratio as an indicator of the oxidation state of amber glasses.

2. Experimental

YSZ sensors were prepared by blending 91 g of YSZ (TOSOH®, TZ-8Y) with 50 cm^3 of a solution 0.01M $NaNO_3$ and 3.5 cm^3 of ammonium polyacrylate as dispersant. The body of the sensor was prepared by slip-casting in a plaster of Paris mold, followed by sintering in air at 1873 K for 2 h. The sensor was shaped in the form of an open-ended tube 5 cm long with an outside diameter of 8 mm.

The YSZ tubes were coated over their entire surfaces with Pt electrode films using a horizontal hot-wall MOCVD apparatus, which has been described elsewhere.[10] The Pt films were carefully removed from the open edge of the tubes with 400-grade emery paper in order to form the working electrode on the external surface and the reference electrode on the internal surface of the tubes. Platinum-acetylacetonate [$(CH_3$-$COCHCO$-$CH_3)_2Pt$] was used as the precursor and its vapors were carried by an argon gas flow to the reactor chamber. Porous Pt films were obtained under the following deposition conditions: precursor temperature, T_{prec} = 443 K; deposition temperature, T_{dep} = 673 K; total gas pressure, P_{tot} = 133 Pa. The YSZ-based tubular sensor for detecting oxygen in glass is shown schematically in Figure 1.

The electrochemical properties of Pt electrode films were investigated by impedance spectroscopy over the frequency range of 10^5–10^{-2} Hz using a Solartron 1255 frequency response analyzer from 573 to 1073 K in air.

Six glasses of different compositions were used for the determination of the oxygen activity. Table 1 shows the final compositions of these glasses in mass %. The last row of this Table shows the initial amount of carbon that was used for preparing each glass. R_2O represents the content of Na_2O plus K_2O. In mullite crucibles, 100 g of glass was melted. Each glass was kept at 1773 K for 2 h to homogenize the composition. Then, the glass was maintained for 1 h at each test temperature (1473, 1573 and 1673 K). The top of the furnace

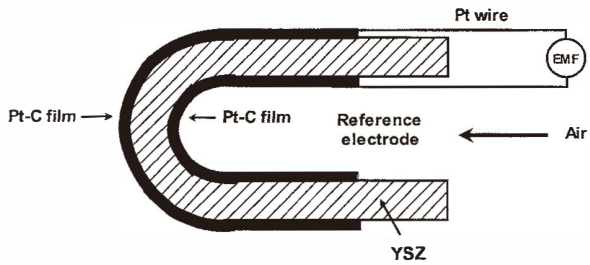

Fig. 1. Cross-sectional view of the YSZ-based sensor with Pt electrode films prepared by MOCVD.

Table 1
Composition of investigated glasses (in mass %).

	GLASS I	G-2	G-3	G-4	G-5	G-6
SiO_2	69.05	75.99	70.98	71.94	71.92	73.02
Na_2O	19.69	15.57	13.23	14.43	14.46	13.72
K_2O	1.55	0.94	0.61	0.64	0.66	0.82
SO_3	0.17	0.09	0.04	0.13	0.07	0.04
FeO	0.324	0.266	0.295	0.277	0.252	0.252
Fe_2O_3	0.595	0.457	0.396	0.387	0.371	0.345
CaO	3.04	2.80	11.48	9.54	9.42	8.41
MgO	0.13	0.10	0.38	0.24	0.32	0.30
Al_2O_3	5.17	3.38	2.33	2.15	2.26	2.68
Cr_2O_3	0.002	0.004	0.003	0.002	0.003	0.005
TiO_2	0.163	0.151	0.137	0.146	0.146	0.150
R_2O	21.24	16.51	13.84	15.07	15.12	14.54
C*	0.257	0.128	0.084	0.078	0.041	0.042

* g C/ 100 g of initial glass

was covered with a ceramic plate and nitrogen gas was introduced from the top of the furnace at a flow rate of 4 L min^{-1} in order to maintain an inert atmosphere above the molten glass. In these experiments the reference electrode was flushed with air and temperature was measured with a type R thermocouple (Pt-Pt, 13%Rh). Figure 2 shows the schematic diagram of the apparatus used to measure the oxygen activity with the YSZ oxygen sensor.

The measurement of oxygen activity is based on the use of the YSZ electrochemical cell which can be represented as:

$$Pt \mid O_2(glass) \mid \mid ZrO_2\,(Y_2O_3) \mid \mid O_2(air) \mid Pt. \qquad (1)$$

When immersed in molten glass, the cell produces an EMF as a result of the difference in oxygen activity between the two sides of the solid electrolyte, according to Nernst's law:

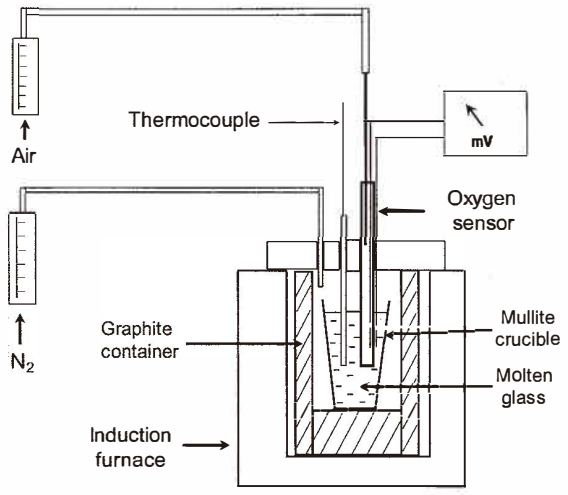

Fig. 2. Schematic diagram of the apparatus used for measuring the oxygen activity in the molten glasses.

$$\mathrm{EMF} = \frac{RT}{4F} \ln \left(\frac{pO_{2\,(\mathrm{glass})}}{pO_{2(\mathrm{air})}} \right), \tag{2}$$

where $pO_{2(air)}$ is the oxygen partial pressure of the reference electrode, $pO_{2(glass)}$ is the oxygen partial pressure in the glass, T is the absolute temperature, R is the gas constant and F is the Faraday constant. The oxidation-reduction reaction in glass may be represented by the following expression:

$$4FeO + O_2 = 2Fe_2O_3 . \tag{3}$$

If the ferric oxide is represented as $FeO_{1.5}$ one obtains:

$$4FeO + O_2 = 4FeO_{1.5} . \tag{4}$$

The Gibbs energy of reaction (4) can be expressed as:

$$\Delta g^{\circ} = -RT \ln \left(\frac{(a_{FeO_{1.5}})^4}{(a_{FeO})^4 [pO_2]} \right). \tag{5}$$

Equation (5) can be changed to

$$\left(\frac{a_{FeO}}{a_{FeO_{1.5}}} \right) = \left[\frac{1}{pO_2} \exp\left(\frac{\Delta g^\circ}{R\,T} \right) \right]^{1/4} \quad (6)$$

The standard Gibbs energy of reaction (4), calculated by the FACT thermodynamic system,[11] is given as:

$\Delta g^\circ = -213434$ J/mol at T = 1473 K

$\Delta g^\circ = -189891$ J/mol at T = 1573 K

$\Delta g^\circ = -164065$ J/mol at T = 1673 K.

3. Results and Analysis

Figure 3 shows the A.C. impedance spectrum in air at 723 K for Pt electrode films prepared by MOCVD on YSZ substrate. The results were analyzed by using three components; i.e., bulk, grain boundary and an interfacial reaction or diffusion limited process. The small semicircle at high frequency was attributed to the bulk response due to a small capacitance (10^{-12} F). The large semicircle in the low frequency region was associated to the charge transfer reactions at the electrode/electrolyte interface. The interfacial reaction component yielded capacitance values in the range of 10^{-7}–10^{-6} F. The grain boundary effect was too small to be resolved at 723 K.

Figure 4 shows the Arrhenius plot for the conductivity in relation to the total electrode resistance for Pt electrode films prepared by MOCVD on the YSZ substrate. The conductivity depends on the physical dimensions of the electrode; in this work we prepared Pt films of about 600 nm thickness. The total electrode resistance is represented by the charge transfer component. Pt films exhibit a higher conductivity than conventional Pt

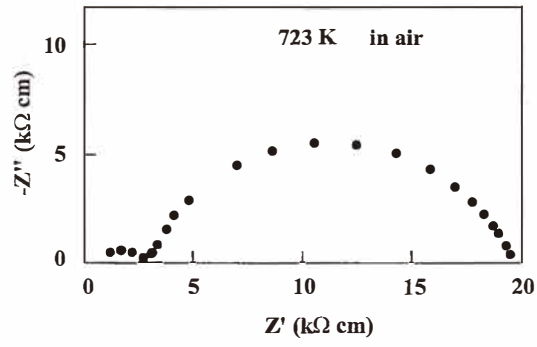

Fig. 3. Impedance spectrum at 723 K of Pt electrode films deposited on YSZ substrate.

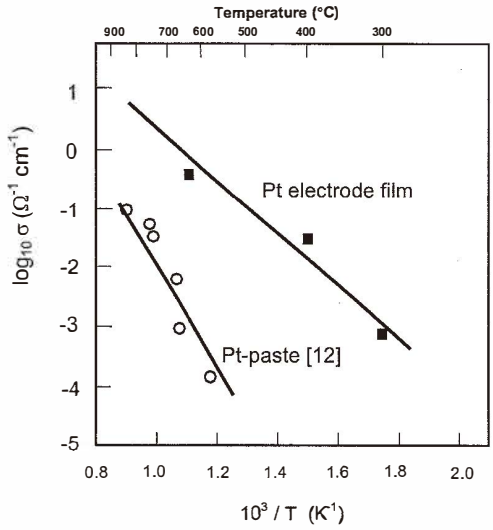

Fig. 4. Arrhenius plots for the conductivity in relation to the total electrode resistance for MOCVD-Pt- and Pt-paste-based electrodes.[12]

paste electrodes at temperatures below 1173 K.[12] Previous Auger results have shown that Pt films prepared by MOCVD contain carbon impurities.[10] It is expected that the carbon content in the film will be eliminated during the preheating step of the sensor. Thus, at the test temperatures (1473–1673 K) the Pt electrode film will contain only a porous Pt film with high conductivity and catalytic activity. In the present work, the working and reference electrodes of the oxygen sensor utilized MOCVD Pt films with superior electrochemical performance to promote the equilibrium in the cell. This enabled the determination of the level of oxygen activity based on the Nernstian response of the sensor.

The activities of FeO and Fe_2O_3 depend on the oxygen activity and can be determined from the equilibrium reaction (3). Simon and Mergler[3] have shown that the amounts of iron oxides in the glass are so small that the activities can be assumed to be equal to the molar fractions: $a_{FeO} = X_{FeO}$ and $a_{Fe2O3} = X_{Fe2O3}$. The ferric oxide can also be represented as $FeO_{1.5}$ according to the expression:

$$FeO_{1.5} = 1/2\ Fe_2O_3. \tag{7}$$

The activity of the ferric oxide represented as $FeO_{1.5}$ can be calculated by the following expression[13]:

$$a\ FeO_{1.5} = (a\ Fe_2O_3)^{1/2}. \tag{8}$$

Then, the final chemical composition can be used to estimate the iron activity ratio as follows:

$$\frac{a\,\mathrm{FeO}}{a\,\mathrm{FeO_{1.5}}} = \frac{\mathrm{X\,FeO}}{(\mathrm{X\,Fe_2O_3})^{1/2}}. \tag{9}$$

Table 2 summarizes the final mole fraction of FeO and Fe_2O_3, together with the activity ratio after cooling, as calculated by (9).

Figure 5 shows the typical pO_2 curves estimated from the sensor output EMF at the test temperatures for glass number 1. The sensors had a response time of approximately 3 s and the EMF stabilized in less than 2 min at all temperatures. No significant difference in the response time was observed among the test temperatures. The fact that the response time was so short in the experiments was attributed to the Pt electrode films deposited on YSZ which increased the electrode conductivity of the sensors compared with that of conventional YSZ sensors.

Table 3 shows the activity ratios determined from the electrochemical measurements at each test temperature. To make the results clearer, the activity ratio calculated at room

Table 2
Mole fraction of the iron oxides and the activity ratio calculated from the chemical composition of the glasses.

Glass Number	X FeO	X Fe_2O_3	aFeO/$a$$FeO_{1.5}$
1	0.00284	0.00232	0.0590
2	0.00230	0.00176	0.0548
3	0.00252	0.00150	0.0650
4	0.00237	0.00147	0.0618
5	0.00216	0.00141	0.0575
6	0.00216	0.00132	0.0594

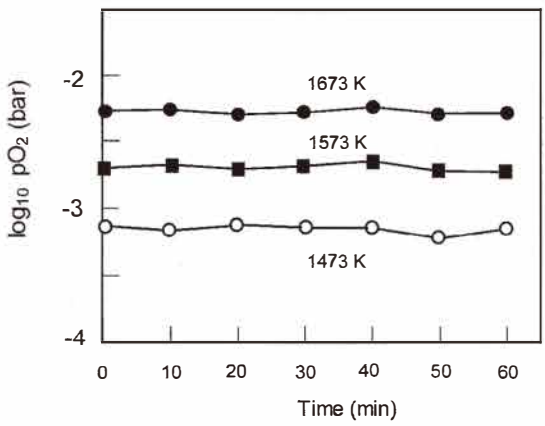

Fig. 5. Oxygen potential in glass 1 as a function of elapsed time.

temperature is also included in Table 3. The activity ratios calculated by the EMF and the FeO-$FeO_{1.5}$ equilibrium reaction are in good agreement with those obtained from the chemical composition. However, a strict comparison reveals some discrepancy in the magnitudes because the FeO-Fe_2O_3 equilibrium in glass changed during cooling. It must be stressed that the sulfur contents in all of the glasses were almost the same and the effect on the FeO-Fe_2O_3 equilibrium can be neglected.

The oxidation-reduction equilibrium in the system moves towards the reduced side with increasing the temperature of the molten glass as expected from the plot of the Gibbs free energy of reactions vs temperature (Ellingham diagram)[14] where the more oxidized species are less stable at higher temperatures. Figure 6 shows that $\log_{10}[a\mathrm{FeO}_{1.5}/a\mathrm{FeO}]$ is linearly dependent on 1/T which is in agreement with the results obtained by Paul for glasses of similar composition.[15]

A clear correlation was found between the oxygen potential in the melt, $pO_{2(\mathrm{glass})}$, and the R_2O/C parameter (where $R_2O = Na_2O+K_2O$ in the final composition of glass and C is the carbon content before the melting of the glass). It is clear that alkaline oxides and carbon play completely different roles in the glass system. Na_2O and K_2O are considered as strong basic oxides, which donate O^{2-} ions to the system according to:

$$R_2O = 2R^+ + O^{2-}, \quad \text{where R = Na and K.} \tag{10}$$

The alkaline oxides can also produce the depolymerization of the silica structure which can be expressed by a scheme such as[16]:

$$R_2O + \text{Si-O-Si} = \text{Si-O}^{-}\ \ {}^{R^+}\!\!\text{O-Si}^{R^+}. \tag{11}$$

Carbon can react with free oxygen atoms in the glass and reduce the oxygen content in the glass according to:

$$C + O_{(\mathrm{glass})} = CO_{(g)}. \tag{12}$$

Table 3
Mean values of the activity ratios estimated by the oxygen sensor.

Glass Number	$a\mathrm{FeO}/a\mathrm{FeO}_{1.5}$ (1473 K)	$a\mathrm{FeO}/a\mathrm{FeO}_{1.5}$ (1573 K)	$a\mathrm{FeO}/a\mathrm{FeO}_{1.5}$ (1673 K)	$a\mathrm{FeO}/a\mathrm{FeO}_{1.5}$ (Estimated at room temperature)
1	0.0795	0.1299	0.1991	0.0590
2	0.0592	0.0851	0.1148	0.0548
3	0.0549	0.0776	0.1096	0.0650
4	0.0401	0.0676	0.1047	0.0618
5	0.0282	0.0525	0.0933	0.0575
6	0.0254	0.0489	0.0865	0.0594

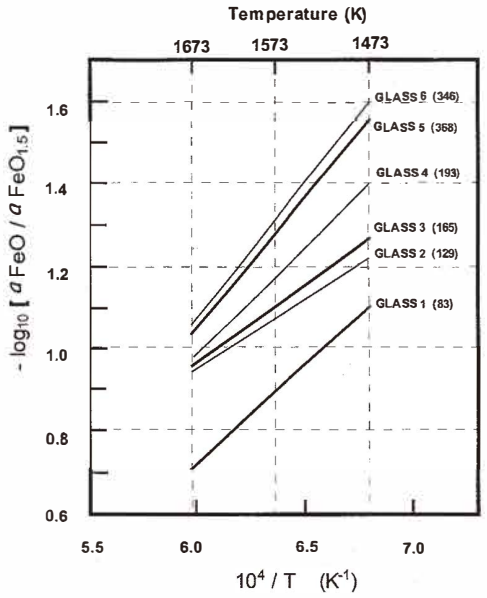

Fig. 6. Effect of temperature on the $a\mathrm{FeO}_{1.5}/a\mathrm{FeO}$ ratio. Numbers in parenthesis represent the $[\mathrm{R_2O/C}]$ parameter.

Thus, it can be expected that the $a\mathrm{FeO}_{1.5}/a\mathrm{FeO}$ ratio may strongly depend on $\mathrm{R_2O/C}$, as shown in Figure 7. This Figure shows that the activity ratio increased with higher values of the $\mathrm{R_2O/C}$ parameter at all of the test temperatures.

It must be stressed that CaO and MgO are also basic oxides and they could be included in a general parameter $(\mathrm{R_2O+MO})/\mathrm{C}$, where R = Na, K; M = Ca, Mg. However, a similar effect on the $a\mathrm{FeO}_{1.5}/a\mathrm{FeO}$ ratio, shown in Figure 7, will be obtained.

4. Conclusions

A sensor employing yttria-stabilized zirconia coated on its surfaces with Pt electrode films deposited by the MOCVD method was used to measure the oxygen activity of amber glasses at temperatures from 1473 K to 1673 K. The MOCVD Pt electrode films improved the response time and the signal stability of the sensors.

The activity ratios calculated by the EMF and the $\mathrm{FeO\text{-}FeO}_{1.5}$ equilibrium reaction are in good agreement with those obtained from the chemical composition. A linear dependence between the $\log_{10}$ $(a\mathrm{FeO}/a\mathrm{FeO}_{1.5})$ and (1/T) was obtained. A direct dependence of the activity ratio $(a\mathrm{FeO}_{1.5}/a\mathrm{FeO})$ on the $\mathrm{R_2O/C}$ (where R = K and Na) was found at all temperatures.

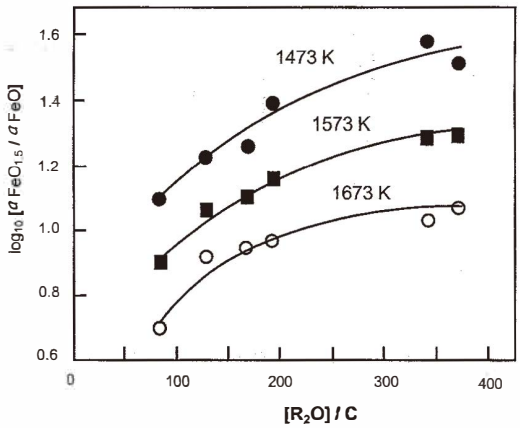

Fig. 7. Effect of the [R_2O/C] parameter on the aFeO$_{1.5}$/aFeO ratio at the test temperatures.

Acknowledgements

The authors wish to thank the Institutions CONACyT, SNI, COFAA and Instituto Politecnico Nacional for their permanent assistance to the Process Metallurgy Group at the ESIQIE Metallurgy and Materials Department.

References

1 A. Lenhart and H. A. Schaffer: Glastech. Ber. **58** (1985) 139.
2 J. W. Matousek: Metall. Trans. and Materials B **25**B (1994) 463.
3 H. M. Simon and K. W. Mergler: Glastech. Ber. **61** (1988) 293.
4 N. Miura, G. Lu and N. Yamazoe: J. Electrochem. Soc. **143** (1996) L33.
5 N. Miura, T. Raisen, G. Lu and N. Yamazoe: J. Electrochem. Soc. **144** (1997) L198.
6 I. Natali-Sora, C. Schmid and C. M. Mori: Proc. of the 17th Riso Int. Symposium on Materials Science: High Temperature Electrochemistry: Ceramics and Metals, Riso National Laboratory, Roskilde, Denmark (1996) p. 369.
7 A. Sharma and P. D. Pacey: J. Electrochem. Soc. **140** (1993) 2302.
8 W. H. Manring and G. M. Diken: J. Non-Crystalline Solids **38** (1980) 813.
9 F. W. Krämer: Glastech. Ber. **64** (1991) 71.
10 T. Goto, R. Vargas and T. Hirai: J. de Phys. IV C**3-3** (1993) 701.
11 W. T. Thompson, C. W. Bale and A. D. Pelton: F*A*C*T-Facility for the Analysis of Chemical Thermodynamics, User's Manual, (1999).
12 S. P. S. Badwal and H.J.De Bruin: Phys. Stat. Sol. **54** (1979) 261.
13 C. H. P. Lupis: Chemical Thermodynamics of Materials, Prentice Hall, Inc., New Jersey, (1983) p. 342.
14 H. J. T. Ellingham: Journal of the Society of Chemical Industry **63** (1944) 125.
15 A. Paul: Journal of Non-Crystalline Solids **71** (1985) 269.
16 J. J. Moore: Chemical Metallurgy, 2nd Edition, Ed. Butterworth & Co., London (1990) p. 152.